Effect of O_2 Flow Concentration during Reactive Sputtering of Ni Oxide Thin Films on Their Electrochemical and Electrochromic Properties in Aqueous Acidic and Basic Electrolyte Solutions

Yoshio Abe[1,2], Se-Hee Lee[1], Esra Ozkan Zayim[1,3], C. Edwin Tracy[1], J. Roland Pitts[1] and Satyen K. Deb[1]

[1]Basic Sciences, National Renewable Energy Laboratory, Golden, CO 80401, U.S.A.

[2]Department of Materials Science, Kitami Institute of Technology, Kitami, Hokkaido 090-8507, Japan

[3]Department of Physics, Istanbul Technical University, Maslak, Istanbul 34469, Turkey

Thin films of Ni oxide were deposited by reactive sputtering in argon/oxygen gas mixtures using O_2 flow concentrations ranging from 6 to 100% and their electrochemical and electrochromic properties were examined using dilute acidic (1 M KCl + 0.5 mM H_2SO_4) and basic (1 M KOH) aqueous electrolyte solutions. An electrochromic coloration efficiency of 32 ± 5 cm^2/C was obtained for all the Ni oxide films regardless of O_2 concentration in both KCl+H_2SO_4 and KOH. The charge capacity and resultant change in the optical density of the Ni oxide films increased with O_2 concentration owing to a decrease in crystal grain size and the resultant increase in the active surface area of the NiO crystal grains. Although the interfacial capacitances of the Ni oxide films in KCl+H_2SO_4 are 2–3 times less than those in KOH, a maximum change in optical density of 0.57 was obtained in KCl+H_2SO_4 for a fine-grained Ni oxide film with a thickness of 400 nm sputtered in 100% O_2.

KEYWORDS: Ni oxide, reactive sputtering, electrochromism, electrolyte, coloration efficiency

1. Introduction

Electrochromic (EC) materials can change their optical properties (darken and lighten) by the application of a small reversible dc voltage. The operation of inorganic EC devices depends on a reversible electrochemical double injection of ionic/electronic species into the host lattice of multivalent transition metal oxide materials.[1,2] Such EC devices are being developed for applications in "smart" energy-efficient windows, antiglare automobile rearview mirrors, and sunroofs.[3-5] A typical EC device consists of a thin film of EC material, an ion storage layer, and an ion-conducting layer sandwiched between two transparent conducting oxide layers.

One of the most important design criteria for an EC device is the proper choice of the ion-conducting layer. Aqueous solutions, nonaqueous solutions, and solid-state electrolytes have been used for ion conduction.[2] Compared with nonaqueous solutions and solid-state electrolytes, aqueous solutions generally have higher ionic conductivities, which contribute to a reduction in switching times and fast optical response. Most of the aqueous solutions cited in the literature are acid solutions for WO_3 and MoO_3 (cathodic EC materials) or alkaline solutions for NiO and CoO (anodic EC materials).[2] A complementary EC device employs a cathodically coloring film as an EC layer and an anodically coloring film as an ion storage layer to improve EC coloration efficiency. To combine WO_3 films (which are unstable in basic electrolyte solutions) with NiO films using aqueous electrolyte solutions, it is necessary to determine the EC properties of NiO films in nonalkaline solutions. Recently, Lee *et al.*[6] have reported on the electrochemical and EC properties of NiO / Ta_2O_5 nanocomposites using neutral KCl aqueous solutions. Our recent preliminary results[7] on the EC properties of sputtered Ni oxide thin films showed a high coloration efficiency (approximately 30 mC/cm^2) in KCl and were comparable to that in alkaline electrolytes. Reports on the EC properties of NiO films in acidic electrolytes are few, because the Pourbaix diagram[8] indicates that NiO is thermodynamically unstable in acidic aqueous solutions. However, we found that Ni oxide thin films show a higher optical density change in acidic KCl+H_2SO_4 aqueous electrolytes than that in neutral KCl aqueous solutions, and no remarkable degradation in charge capacity was observed up to 100 cycles.[9] It is supposed that the dissolution rate of

NiO is very low at least in diluted acidic solutions, and it is possible to apply NiO to complementary EC devices using aqueous electrolyte solutions.

The oxygen content of the sputter gas mixture is an important processing variable affecting the electrochemical and electrochromic properties of Ni oxide films prepared by reactive sputtering. [10-18] In this study, the O_2 flow concentration of the Ar/O_2 sputter gas was varied as a parameter to study the optical modulation characteristics of Ni oxide EC films. The electrochemical and electrochromic properties of the Ni oxide films in $KCl+H_2SO_4$ diluted acid solution are compared with those measured in aqueous KOH solution, which is one of the most widely used alkaline electrolytes for Ni oxide.

2. Experimental Procedure

Ni oxide thin films with thicknesses of 400 nm were concurrently deposited on glass substrates coated with a transparent conducting layer of F-doped SnO_2 (FTO) for electrochemical and EC characterizations and on plain glass substrates for structural analysis. A Ni target was sputtered in Ar/O_2 atmosphere using a radio-frequency (RF) magnetron sputtering system to deposit Ni oxide films, as reported in a previous paper.[7] Oxygen flow concentration, $[O_2/(Ar+O_2)] \times 100\%$, was varied as a parameter from 6 to 100%. Total gas flow rate, RF power and substrate-target distance were standardized to 30 standard cubic centimeters per minute (sccm), 60 W and 5 cm, respectively. Total sputtering gas pressure was consistently maintained at 1.5 Pa with no intentional substrate heating. The deposition rates for depositing Ni oxide films decreased from 4 to 2 nm/min with increasing O_2 flow concentration (across 6 to 100%).

The crystal structure was characterized by X-ray diffraction (XRD) analysis using Cu-Kα radiation. Cyclic voltammetry (CV) and *in situ* optical measurements were carried out in 1 M KCl with approximately 0.5 mM H_2SO_4 and 1 M KOH aqueous solutions using Ag/AgCl and Pt as reference and counter electrodes, respectively. The diluted acid solution was used for the measurements because we have examined the EC properties of Ni oxide thin films in $KCl+H_2SO_4$ mixed solutions with H_2SO_4 concentrations of 0–50 mM, and a maximum charge capacity and a maximum change in optical density were obtained in the solution (0.5 mM H_2SO_4 + 1 M KCl).[9] *In situ* optical modulation was measured using a laser diode at a 670 nm wavelength, and *ex situ*

transmittance spectra after bleaching and coloring were measured using a spectrophotometer.

3. Results and Discussion

The effects of O_2 flow concentration in sputter gas on the structure of the Ni oxide thin films deposited on glass substrates were studied by XRD analysis. As shown in Fig. 1, crystalline diffraction peaks due to cubic NiO (rock salt) are clearly evident for the sample deposited at an O_2 concentration of 6%. However, peak intensity decreases and peak width increases with increasing O_2 concentration and distinct diffraction peaks are minimal for the film deposited with 100% O_2. The crystal grain size of the Ni oxide film deposited at 6% O_2 was estimated to be 15–30 nm using Scherrer's formula,[19] and crystal grain size decreases with increasing O_2 flow ratio.

The electrochemical properties of these Ni oxide films have also been studied by CV analysis in 1 M KCl + 0.5 mM H_2SO_4 and 1 M KOH aqueous solutions in voltage scan ranges of 0 to 1.0 V and -0.5 to 0.5 V, respectively. Upon initial cycling, current density increases, and stabilizes after 10 or 20 cycles, similar to the results reported in previous papers.[20,21] The CV curves of the Ni oxide films in KCl+H_2SO_4 and KOH using a voltage scan rate of 10 mV/s after stabilization are shown in Figs. 2(a) and 2(b), respectively. The 6% O_2 concentration CV curve with KCl+H_2SO_4 for the well-crystallized Ni oxide film (as identified in Fig. 1) is pseudocapacitive in nature (i.e., mirror image cathodic and anodic CV curves with a rectangular shape) and two broad reversible peaks (located at approximately 0.6 V on oxidation and 0.5 V on reduction) are observed. The CV profiles of the Ni oxide films deposited at O_2 concentrations of 50 and 100% became progressively more slanted and deformed with respect to the rectangular pseudocapacitive shape, which is indicative of slow ion diffusion. With a KOH electrolyte, redox peaks for all three samples are clearly evident at 0.39–0.4 V and 0.20–0.25 V for anodic and cathodic scans, respectively. The pseudocapacitive profile of these Ni oxide films in KOH is considered to be caused by the reaction [22]

$$NiO + OH^- \leftrightarrow NiOOH + e^-. \quad (1)$$

Some researchers have claimed that H^+ ions also contribute to the reaction.[23] The redox peaks in KOH are thought to be due to the following reactions of $Ni(OH)_2$ [24,25] which are formed at the surface of the NiO grains during the initial cycling[26] :

$$Ni(OH)_2 \leftrightarrow NiOOH + H^+ + e^- \qquad (2A)$$

or

$$Ni(OH)_2 + OH^- \leftrightarrow NiOOH + H_2O + e^-. \qquad (2B)$$

Although the electrochemical reaction mechanisms in KCl+H_2SO_4 are not clear, it seems that both K^+ adsorption and H^+ insertion are involved in the electrochemical reaction of NiO films in KCl + H_2SO_4 electrolyte. It is speculated that the adsorption and desorption of K^+ ions at the surface of NiO nanocrystals induce the pseudocapacitive properties and that the intercalation and deintercalation of H^+ ions into and out of NiO nanocrystals induce the redox peaks.[9] The current densities of the CV curves, regardless of electrolyte type, increase with O_2 flow concentration indicating a progressive increase in the charge capacity of the Ni oxide films.

Figure 3(a) shows the effect of O_2 flow concentration on the interfacial capacitance of the Ni oxide films in KCl+H_2SO_4 and KOH at a voltage scan rate of 10 mV/s. The interfacial capacitance was calculated from the CV curves using the formula $C=I_{av}/(dV/dt)$, where I_{av} is the average current density and dV/dt is the voltage scan rate. Since current-voltage response is voltage dependent unlike an ideal capacitor, we used the average charging and discharging currents for the calculation. The interfacial capacitances of the NiO films increase with O_2 flow concentration in both KCl+H_2SO_4 and KOH; however, the interfacial capacitances in KCl+H_2SO_4 are 2–3 times smaller than those measured in KOH. Pseudocapacitance is an interfacial phenomenon and a large surface area enhances its charge storage capability. Therefore, the increase in interfacial capacitance as a function of O_2 concentration shown in Fig. 3(a) is most likely due to the progressively decreasing crystal grain sizes of the NiO films (inferred from the XRD data in Fig. 1). A more extensive study is required to identify the ion species responsible for the electrochemical reactions in KCl+H_2SO_4.

Figure 3(b) shows the effect of voltage scan rate on the interfacial capacitance of the Ni oxide films in both KCl+H_2SO_4 and KOH electrolytes. The interfacial capacitance of the well-crystallized Ni oxide film deposited at 6% O_2 concentration changes slightly

with voltage scan rate (regardless of electrolyte type), which is the behavior of an ideal capacitor. Despite the larger interfacial capacitances for the finer-grained Ni oxide films deposited at 50 and 100% O_2 concentrations, these interfacial capacitances decrease with increasing voltage scan rate in both KCl+H_2SO_4 and KOH. Most probably the length of the diffusion path for ion migration increases with decreasing crystal grain size, which in turn causes a decrease in ion mobility. The stoichiometry of the Ni oxide films (ratio of Ni^{2+}/Ni^{3+}) may also affect capacitance.[13,14,17,18]

Figure 4 shows the transmittance spectra of an FTO-coated glass substrate and Ni oxide films deposited on similar substrates at an O_2 flow concentration of 30%. The films were colored by applying a constant voltage of 1 V (vs Ag/AgCl reference electrode) for 5 min. The bleached state transmittance spectra were measured after bleaching at 0 V vs Ag/AgCl for 5 min. The bleached films exhibited a light yellow tint and the colored films appeared dark brown. The colored and bleached transmittance spectra in KCl+H_2SO_4 are basically similar in character to those in KOH although they have a slightly higher transmittance.

Figure 5 shows the change in optical density [$\Delta OD = \log_{10} (T_b/T_c)$, where T_b and T_c are bleached and colored transmittance, respectively] of the Ni oxide films deposited at O_2 flow concentrations of 6, 50, and 100% in KCl+H_2SO_4 as a function of charge density (ΔQ). To avoid the potential effects of irreversible side reactions (such as gas evolution), optical density was measured during the negative scan (bleaching) from 1.0 to 0 V vs Ag/AgCl with a constant current density of 20 μA/cm (galvanostatic measurement).[27] The change in optical density for all NiO samples increases almost linearly with charge density, regardless of O_2 flow concentration. The maximum optical density change was 0.2 at a charge density of 6.8 mC/cm^2 for the well-crystallized Ni oxide film deposited at the 6% O_2 concentration. However, the change in optical density for the fine-grained film deposited at the 100% O_2 concentration increases up to 0.57 and corresponds to an increase in charge capacity of 18 mC/cm^2. EC coloration efficiency [$\Delta(OD)/ \Delta Q$] is shown as a function of O_2 flow concentration for the NiO samples in Fig. 6. Nearly constant EC coloration efficiencies on the order of 32 ± 5 cm^2/C were found for all of the films regardless of O_2 flow concentration in both KCl+H_2SO_4 and KOH. These

values are comparable to those reported for sputtered Ni oxide thin films in KOH and NaOH alkaline electrolytes (31–36 cm^2/C at wavelengths of 550–633 nm).[11,13,28,29]

Since the colored and bleached transmittance spectra and coloration efficiencies obtained in $KCl+H_2SO_4$ diluted acid electrolytes are similar to those obtained in KOH alkaline electrolytes, we can conjecture that the coloration mechanisms of the Ni oxide films in both electrolyte are similar, i.e., the valence changes of Ni ions between Ni^{2+} (bleached) and Ni^{3+} (colored).[23,25] The long-time stability of the Ni oxide films in the diluted acidic solutions should be studied in the future.

4. Conclusions

Various Ni oxide thin films (400 nm thick) were deposited by reactive sputtering in an Ar/O_2 gas mixture with O_2 flow concentration ranging from 6–100%. The electrochemical and electrochromic properties of the films were measured in $KCl+H_2SO_4$ diluted acid and KOH alkaline solutions using various voltage scan rates. With increasing O_2 flow concentration, the crystal grain size of NiO decreases as shown by XRD analysis. Interfacial capacitances progressively increase for the finer-grained Ni oxide films deposited with higher O_2 flow concentrations. The increases in the active surface area of the finer-grained NiO crystals are considered to be the primary reason for the increases in interfacial capacitances. All Ni oxide films exhibited a coloration efficiency of 32 ± 5 cm^2/C in both $KCl+H_2SO_4$ and KOH regardless of O_2 flow concentration in the sputter gas. In general, Ni oxide films deposited with increasing O_2 flow concentrations exhibited progressively increased changes in optical density.

1) S. K. Deb: Philos. Mag. **27** (1973) 801.

2) C. G. Granqvist: *Handbook of Inorganic Electrochemical Materials* (Elsevier, New York, 1995).

3) J. Nagai, G. D. McMeeking and Y. Saitoh: Sol. Energy Mater. Sol. Cells **56** (1999) 309.

4) S. K. Deb, S.-H. Lee, C. E. Tracy, J. R. Pitts, B. A. Gregg and H. M. Branz: Electrochim. Acta **46** (2001) 2125.

5) C. M. Lampert: Sol. Energy Mater. Sol. Cells **76** (2003) 489.

6) S.-H. Lee, C. E. Tracy, Y. Yan, J. R. Pitts and S. K. Deb: Electrochem. Solid-State Lett. **8** (2005) A188.

7) Y. Abe, S.-H. Lee, E. Ozkan-Zayim, C. E. Tracy, J. R. Pitts and S. K. Deb: Electrochem. Solid-State Lett. **9** (2006) G17.

8) M. Pourbaix: *Atlas of Electrochemical Equilibria in Aqueous Solutions* (National Association of Corrosion Engineers, Houston, 1974) 2nd ed. Sect. 12.3, p. 330.

9) Y. Abe, S.-H. Lee, C. E. Tracy, J. R. Pitts and S. K. Deb: Electrochem. Solid-State Lett. **9** (2006) J31.

10) S. Yamada, T. Yoshioka, M. Miyashita, K. Urabe and M. Kitao: J. Appl. Phys. **63** (1988) 2116.

11) D. A. Wruck, M. A. Dixon, M. Rubin and S. N. Bogy: J. Vac. Sci. Technol. A **9** (1991) 2170.

12) K. Yoshimura, T. Miki and S. Tanemura: Jpn. J. Appl. Phys. **34** (1995) 2440.

13) F. F. Ferreira, M. H. Tabacniks, M. C. A. Fantini, I. C. Faria and A. Gorenstein: Solid State Ionics **86-88** (1996) 971.

14) I. C. Faria, M. Kleinke, A. Gorenstein, M. C. A. Fantini and M. H. Tabacniks: J. Electrochem. Soc. **145** (1998) 235.

15) K.-S. Ahn, Y.-C. Nah, J.-H. Yum and Y.-E. Sung: Jpn. J. Appl. Phys. **41** (2002) L212.

16) E. Avendaño, A. Azens, G. A. Niklasson and C. G. Granqvist: J. Solid State Electrochem. **8** (2003) 37.

17) K.-S. Ahn, Y.-C. Nah and Y.-E. Sung: Solid State Ionics **156** (2003) 433.

18) S.-H. Lee, C. E. Tracy and J. R. Pitts: Electrochem. Solid-State Lett. **7** (2004) A299.

19) B. D. Cullity and S. R. Stock: *Elements of X-ray Diffraction* (Prentice Hall, Upper Saddle River, 2001) 3rd ed., p. 170.

20) S. R. Jiang, B. X. Feng, P. X. Yan, X. M. Cai and S. Y. Lu: Appl. Surf. Sci. **174** (2001) 125.

21) I. Bouessay, A. Rougier, B. Beaudoin and J. B. Leriche: Appl. Surf. Sci. **186** (2002) 490.

22) V. Srinivasan and J. W. Weidner: J. Electrochem. Soc. **147** (2000) 880.

23) K.-W. Nam and K.-B. Kim: J. Electrochem. Soc. **149** (2002) A346.

24) P. C. Yu, G. Nazri and C. M. Lampert: Sol. Energy Mater. **16** (1987) 1.

25) M. K. Carpenter, R. S. Conell and D. A. Corrigan: Sol. Energy Mater. **16** (1987) 333.

26) I. Bouessay, A. Rougier, P. Poizot, J. Moscovici, A. Michalowicz and J.-M. Tarascon: Electrochim. Acta **50** (2005) 3737.

27) E. Avendaño, A. Azens, G. A. Niklasson and C. G. Granqvist: Sol. Energy Mater. Sol. Cells **84** (2004) 337.

28) M. Kitao, K. Izawa, K. Urabe, T. Komatsu, S. Kuwano and S. Yamada: Jpn. J. Appl. Phys. **33** (1994) 6656.

29) K.-S. Ahn, Y.-C. Nah and Y.-E. Sung: Jpn. J. Appl. Phys. **41** (2002) L533.

Figure caption

Fig. 1. X-ray diffraction patterns of Ni oxide films deposited on glass substrates as function of O_2 flow concentration in Ar/O_2 sputter gas (6, 17, 50, 100%).

Fig. 2. Cyclic voltammogram images measured in (a) 1 M KCl + 0.5 mM H_2SO_4 and (b) 1 M KOH aqueous electrolytes for Ni oxide thin films deposited at various O_2 flow concentrations in sputter gas (6, 50, and 100%). Voltage scan rates were 10 mV/s.

Fig. 3. Interfacial capacitances of Ni oxide films measured in 1 M KCl + 0.5 mM H_2SO_4 and 1 M KOH (a) as function of O_2 flow concentration in Ar/O_2 sputter gas at fixed voltage scan rate of 10 mV/s and (b) as function of various voltage scan rates. Open and closed squares indicate the interfacial capacitances measured in KCl+H_2SO_4 and KOH, respectively.

Fig. 4. Transmittance spectra of FTO-coated glass substrate and Ni oxide thin films deposited on similar substrates with O_2 flow concentration of 30% in sputter gas. The coloration and bleaching of the Ni oxide films were measured using KCl+H_2SO_4 and KOH aqueous electrolytes.

Fig. 5. Optical density changes of Ni oxide thin films (deposited at O_2 flow concentrations of 6, 50, and 100%) as functions of charge density during bleaching. Optical density was measured *in situ* in 1 M KCl + 0.5 mM H_2SO_4 at a wavelength of 670 nm and current density was kept constant at 20 $\mu A/cm^2$.

Fig. 6. EC coloration efficiencies of Ni oxide films as functions of O_2 flow concentration in sputter gas. Optical density was measured *in situ* during bleaching in 1 M KCl + 0.5 mM H_2SO_4 (open squares) and 1 M KOH (close squares) at a wavelength of 670 nm. Current density was kept constant at 20 $\mu A/cm^2$.

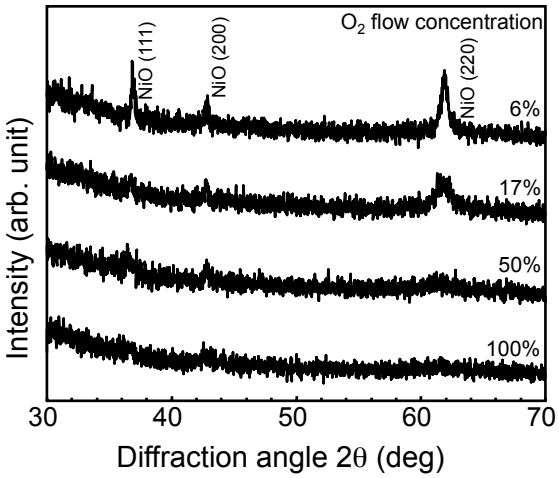
O2 flow concentration
NiO (111)
NiO (200)
NiO (220)
6%
17%
50%
100%
Intensity (arb. unit)
30
40
50
60
70
Diffraction angle 2θ (deg)

Fig. 1

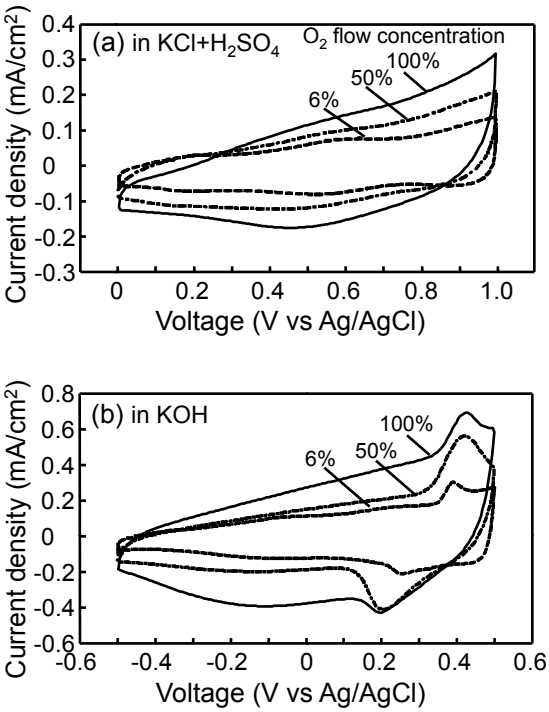
(a) in KCl+H2SO4
O2 flow concentration
100%
50%
6%
Current density (mA/cm2)
0.4
0.3
0.2
0.1
0
-0.1
-0.2
-0.3
0
0.2
0.4
0.6
0.8
1.0
Voltage (V vs Ag/AgCl)
(b) in KOH
100%
50%
6%
Current density (mA/cm2)
0.8
0.6
0.4
0.2
0
-0.2
-0.4
-0.6
-0.6
-0.4
-0.2
0
0.2
0.4
0.6
Voltage (V vs Ag/AgCl)

Fig. 2

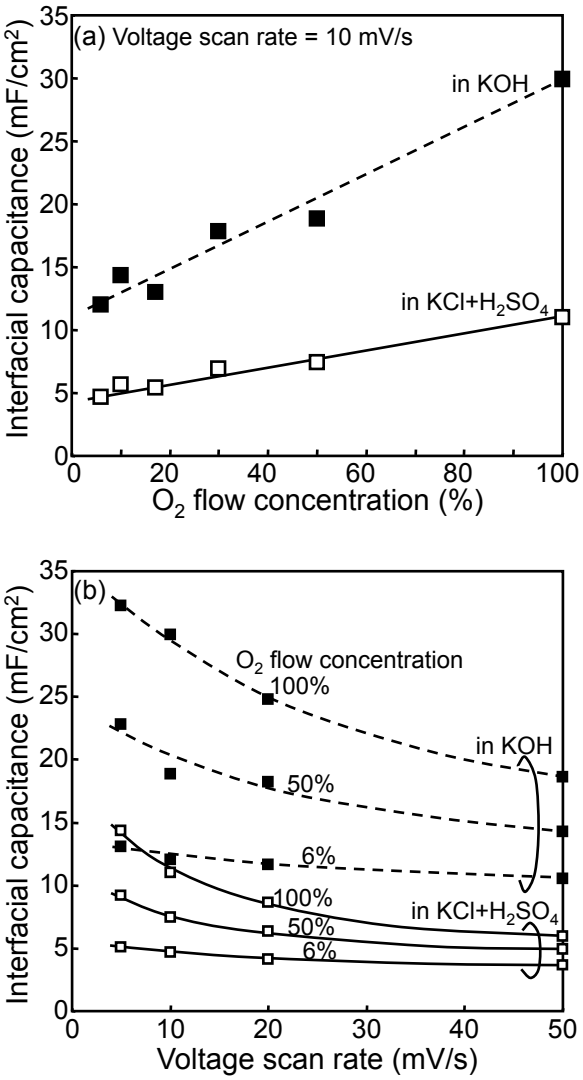
(a) Voltage scan rate = 10 mV/s
in KOH
in KCl+H2SO4
Interfacial capacitance (mF/cm2)
O2 flow concentration (%)
(b)
O2 flow concentration
100%
50%
6%
in KOH
100%
50%
6%
in KCl+H2SO4
Interfacial capacitance (mF/cm2)
Voltage scan rate (mV/s)

Fig. 3

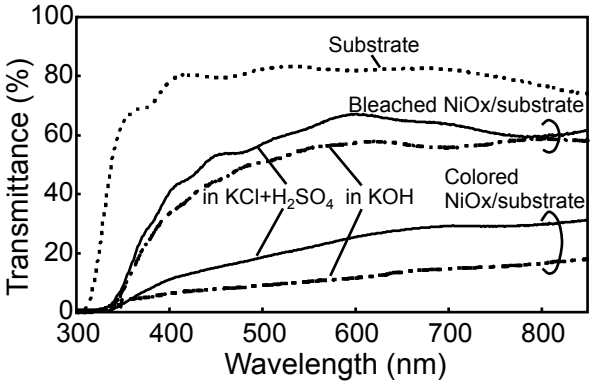
Substrate
Bleached NiOx/substrate
Colored
NiOx/substrate
in KCl+H2SO4
in KOH
Transmittance (%)
Wavelength (nm)
100
80
60
40
20
0
300
400
500
600
700
800

Fig. 4

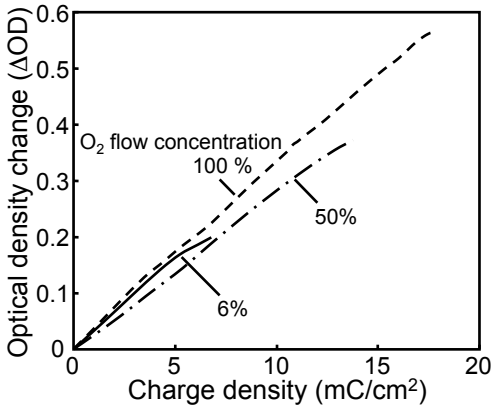
O2 flow concentration
100 %
50%
6%
Optical density change (ΔOD)
Charge density (mC/cm2)
0.6
0.5
0.4
0.3
0.2
0.1
0
0
5
10
15
20

Fig. 5

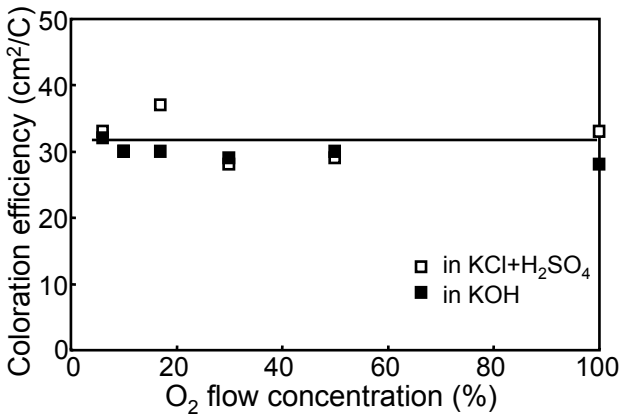
Coloration efficiency (cm²/C)
50
40
30
20
10
0
0
20
40
60
80
100
O2 flow concentration (%)
in KCl+H2SO4
in KOH

Fig. 6